UNIVERSITÀ DEGLI STUDI DI ROMA "TOR VERGATA"

FACOLTA' DI MEDICINA

DOTTORATO DI RICERCA IN FISIOPATOLOGIA SPERIMENTALE

XXI CICLO

Induction of apoptosis in human prostate cancer cells by Insulin-like Growth Factor Binding Protein 3 does not require binding to retinoid X receptor-α

Giovanna Zappalá

A.A. 2008/2009

Tutor: Prof. Massimo Federici

Coordinator: Prof. Renato Lauro

INDEX/TABLE OF CONTENTS

ABSTRACT[1]

IGF binding protein (IGFBP)-3 can induce apoptosis in human prostate cancer cells directly without sequestering IGF-I and -II. The molecular mechanisms responsible for the IGF-independent actions of IGFBP-3 remain unclear. IGFBP-3, a secreted protein, can be internalized and translocate to the nucleus. It binds to the nuclear retinoid X receptor (RXR)-α. Binding to RXR-α has been proposed to be required for IGFBP-3 to induce apoptosis. The present study tests this hypothesis in the PC-3 human prostate cancer cell line. PC-3 cells express RXR-α, and apoptosis is induced by incubation with RXR-specific ligand. A COOH-

[1]The work described in this dissertation has been published in *Endocrinology* 149: 1802-1812, 2008. Reproduced with permission.

terminal region in IGFBP-3 (residues 215–232) contains a nuclear localization signal, and binding domains for RXR-α and heparin (HBD). Different combinations of the 11 amino acids in this region that differ from IGFBP-1, a related IGFBP, which does not localize to the nucleus or bind RXR-α, were mutated to the IGFBP-1 sequence. By confocal imaging, mutation of residues 228-KGRKR-232 in nonsecreted IGFBP-3 diminished its nuclear localization. IGFBP-3 binding to glutathione S-transferase-RXR-α only was lost when all 11 sites were mutated (HBD-11m-IGFBP-3). Expressed nuclear RXR-α did not transport cytoplasmic IGFBP-3 nuclear localization signal mutants that can bind RXR-α to the nucleus even after treatment with RXR ligand. Expressed HBD-11m-IGFBP-3 still induced apoptosis in PC-3 cells in an IGF-independent manner as determined by flow cytometric analysis of Annexin V staining. We conclude that in PC-3 cells, RXR-α is not

required for the nuclear translocation of IGFBP-3 and that IGFBP-3 can induce apoptosis in human prostate cancer cells without binding RXR-α.

INTRODUCTION

IGF BINDING PROTEIN (IGFBP)-3, the most abundant IGFBP in plasma, can inhibit cell proliferation and induce apoptosis by binding to IGF-I and -II to form complexes that prevent the growth factors from activating IGF-I receptors (1, 2). IGFBP-3 also can inhibit growth and induce apoptosis in cells grown in culture by direct mechanisms that do not involve binding IGFs (3-10). IGF-independent growth inhibition has been demonstrated using IGFBP-3 mutants that cannot bind IGF-I or IGF-II (3-7, 11), and in cells that lack IGF-I receptors (8, 9, 10). Expression of an IGFBP-3 mutant that does not bind IGFs inhibited the growth of prostate tumors at late stages of tumorigenesis in a transgenic mouse model *in vivo* (11). The IGF-independent mechanisms by which IGFBP-3 acts directly to induce apoptosis are not well understood. Candidate IGFBP-3 receptors (12-15) and signal transduction pathways (6, 16,

17) have been described, but their physiological significance has not been established. IGFBP-3 is a secreted protein that can be internalized (18, 19) by endocytosis via clathrin-coated pits or caveolin-1-containing lipid rafts (20, 21). It contains a nuclear localization signal (NLS) (22) and can translocate into the nucleus (23-27). The functional significance of nuclear IGFBP-3 remains uncertain because IGFBP-3 mutants that are not concentrated in the nucleus are able to induce apoptosis in breast (28) and prostate (27) cancer cells. However, these results do not exclude the possibility that nuclear localization may play a role in the induction of apoptosis by wild-type (WT) IGFBP-3.

Nuclear action of IGFBP-3 was suggested by the demonstration that it bound to the nuclear retinoid X receptor (RXR)-α (26, 29). Support came from the demonstration that IGFBP-3 also

modulated transcription stimulated by RXR-RXR homodimers or heterodimers of RXR with other nuclear receptor partners, including the retinoic acid receptor (RAR), vitamin D receptor (VDR), and peroxisome proliferator-activated receptor-γ (26, 29, 30). RXR-α homodimers stimulate transcription from RXR response elements (RXREs) after binding RXR-specific ligands (31-33). RXR-α heterodimers increase transcription from response elements that are specific for their receptor partners when they are activated by their specific ligands (34-38). IGFBP-3 modulates transcription stimulated by RXR-RXR homodimers and RXR heterodimers in different ways. It enhances transcription induced by RXR-RXR homodimers (26, 30) but inhibits transcription induced by RXR-RAR and RXR-VDR heterodimers (26, 29, 30), possibly by promoting dissociation of the heterodimers (29).

In addition to IGFBP-3 regulating RXR-α transcriptional activity, RXR-α can regulate cellular responses to IGFBP-3. RXR ligand promoted the colocalization of RXR-α and IGFBP-3 in the nucleus of Los Angeles prostate cancer (LAPC)-4 human prostate cancer cells (26). The fact that RXR ligand enhanced the nuclear localization of IGFBP-3 suggested that RXR-α might be involved in transporting IGFBP-3 to the nucleus. Studies in F9 embryonal carcinoma cells suggested that RXR-α also was involved in the induction of apoptosis by IGFBP-3 because IGFBP-3 could induce apoptosis only in F9 cells that expressed RXR-α (26). The inability of IGFBP-3 to induce apoptosis in RXR-α-null F9 cells was a specific effect because apoptosis could be induced in these cells by the atypical retinoid fenretinide (*N*-[4-hydroxyphenyl]retinamide) (39, 40) or the oxidative stress agent arsenite trioxide (41). Combined with the ability of IGFBP-3 to bind RXR-α, these results

raised the possibility that direct binding of IGFBP-3 to RXR-α might be required for the induction of apoptosis by IGFBP-3 (26). Although IGFBP-3 can induce apoptosis without being concentrated in the nucleus (27), this does not preclude the possibility that binding to RXR-α is involved. RXR-α shuttles between nucleus and cytoplasm (42, 43), so that interaction between IGFBP-3 and RXR-α might occur in the cytoplasm.

The present study addresses two questions: whether RXR-α plays a role in the nuclear localization of IGFBP-3, and whether RXR-α binding to IGFBP-3 is required for IGFBP-3 induction of apoptosis in the PC-3 human prostate cancer cell line. Our approach has been to mutate different combinations of 11 residues in a highly basic COOH-terminal region of IGFBP-3, residues 215–232, that contains a bipartite NLS (22), RXR-α binding site (26), and heparin

binding domain (HBD) (2), to the corresponding sequence of IGFBP-1, a closely related IGFBP (2), which neither localizes to the nucleus nor binds RXR-α (24, 26). We have identified IGFBP-3 mutants that do not localize to the nucleus but are able to bind to RXR-α, and show that they do not translocate from the cytoplasm to the nucleus, even when RXR-α is overexpressed and the cells are treated with RXR ligand. These results do not support the hypothesis that RXR-α can translocate IGFBP-3 to the nucleus. We also show that an IGFBP-3 mutant, which does not bind to RXR-α or localize to the nucleus, is still able to induce apoptosis in PC-3 human prostate cancer cells in an IGF-independent manner, indicating that binding to RXR-α is not a prerequisite for IGFBP-3 to induce apoptosis in human prostate cancer cells.

MATERIAL AND METHODS

Materials

Mouse monoclonal antibody to green fluorescent protein (GFP) was obtained from Covance (Berkeley, CA). Rabbit anti-RAR-γ and rabbit anti-RXR-α were purchased from Santa Cruz Biotechnology, Inc. (Santa Cruz, CA). Horseradish peroxidase (HRP) conjugated to goat anti-glutathione S-transferase (GST) polyclonal antibody (anti-GST-HRP conjugate) was purchased from Amersham Biosciences (Piscataway, NJ). Mouse monoclonal anti-RXR-α antibody was obtained from Chemicon International (Temecula, CA), Alexa Fluor 594 goat antimouse IgG from Molecular Probes-Invitrogen, Carlsbad, CA), rabbit IgG from Sigma-Aldrich (St. Louis, MO), and recombinant human RXR-α from ProteinOne (Bethesda, MD).

A plasmid expressing GST-RXR-α was obtained from David J. Mangelsdorf (Howard Hughes Medical Institute Research Laboratories, The University of Texas Southwestern Medical Center at Dallas, Dallas, TX). Plasmids pCMX and pCMX-RXR-α, and the RXRE-luciferase reporter plasmid thymidine kinase promoter-cellular retinol binding protein II-RXRE-luciferase (TK-CRBPII-Luc) (44, 45) were kindly provided by Kai Ge (NIDDK, NIH).

The RXR-specific ligand LG100268 (referred to as LG268) (46) was synthesized and provided by Melissa Perreira and Craig Thomas (Biotechnology Core, NIDDK). GST was purchased from Upstate Biotechnology (Lake Placid, NY). Glutathione Sepharose-4B Beads were obtained from Amersham Biosciences. Protein A/G Plus Agarose beads were purchased from Santa Cruz

Biotechnology. Annexin V-APC and the general caspase inhibitor, benzyloxycarbonyl (Z)-VAD-fluoromethylketone (fmk), were obtained from BD Biosciences-Pharmingen (San Diego, CA).

Cell cultivation

The PC-3 human prostate cancer cell line was obtained from the American Type Culture Collection (ATCC; Manassas, VA; CRL-1435) and cultured in F12K medium (ATCC) containing 10% fetal bovine serum (FBS) (HyClone Laboratories, Logan, UT) in a humidified atmosphere containing 5% CO_2 at 37 C as previously described (27). LNCaP-FGC human prostate cancer cells (ATCC; CRL-1740) were obtained from Julia Arnold and Marc Blackman (National Center for Complementary and Alternative Medicine, NIH), and cultured in 1:1 DMEM:F12K medium containing 5% FBS (47).

Construction of IGFBP-3 mutants

To study the subcellular distribution, interaction with RXR-α, and proapoptotic activity of WT and mutant IGFBP-3, we transfected human prostate cancer cells with nonsecreted yellow fluorescent protein (YFP)-IGFBP-3 fusion proteins as previously described (27). Constructs expressing nonsecreted fusion proteins were chosen to facilitate the analysis of nucleocytoplasmic distribution by eliminating the need for secreted or exogenous mutant proteins to cross the plasma membrane to reenter the cell (28, 48). PC-3 cells express endogenous IGFBP-3 at low levels (27, 49). Although endogenous and expressed proteins may differ in their nucleocytoplasmic distribution (50) and ability to induce apoptosis (51), we have shown that glycosylated exogenous and secreted

IGFBP-3 induce apoptosis in PC-3 cells (5, 27) like the nonsecreted, nonglycosylated IGFBP-3 used in the present study.

Plasmids in which the mature form of WT human IGFBP-3 (residues 1–264) (52) without its signal peptide, and the NLS mutant YFP-MDGEA-IGFBP-3 (Fig. 1), were fused in-frame to the COOH terminus of YFP in the YFP-C1 vector (BD Biosciences-Clontech, Palo Alto, CA) were previously described (27). Additional mutations in the HBD (Fig. 1) were introduced in WT YFP-IGFBP-3 and YFP-MDGEA-IGFBP-3 using a PCR-based site-directed mutagenesis strategy (QuikChange, Stratagene, La Jolla, CA). First, mutations of K216N-K220H-K221S-K222R were introduced using the sense oligonucleotide: 5'-CCCAACTGTGACAACGGATTTTATCACTCACGGCAGTGTCGC-CTTCC-3' and the complementary antisense oligonucleotide.

The nucleotides that were changed from wild type are *underlined*. Introduction of K216N-K220H-K221S-K222R into YFP-MDGEA-IGFBP-3 generated YFP-HBD-9m-IGFBP-3. Next, the mutations R225E-P226T were introduced into YFP-K216N-K220H-K221S-K222R-IGFBP-3 and YFP-HBD-9m-IGFBP-3 to generate YFP-HBD-6m-IGFBP-3 and YFP-HBD-11m-IGFBP-3, using the oligonucleotides:

5'TATCACTCACGGCAGTGTGAGACTTCCAAAGGCAGGAA GCGGGGC-3' and

5'TATCACTCACGGCAGTGTGAGACTTCCATGGATGGGGA GGCGGGC-3', respectively. The PCR cycling parameters were: 95 C for 30 sec, 95 C for 30 sec (denaturation), 48 C for 1 min (annealing), 68 C for 12 min (21 cycles of elongation), followed by 68 C for 7 min. PCR was followed by digestion of the parental DNA template and transformation into XL-1 Blue Supercompetent

cells (Stratagene). All constructs were confirmed by DNA sequencing. The HBD-11m mutation also was introduced into YFP-6m-IGFBP-3 containing the NH_2-terminal 6m mutation in the IGF-binding site (Ref. 5 and legend to Fig. 1) to generate the double mutant YFP-6m/HBD-11m-IGFBP-3.

Imaging and confocal microscopy

Imaging of different YFP-IGFBP-3 constructs was performed as previously described (53). PC-3 cells (2×10^5 cells per well in a six-well plate; Corning, Inc., Costar, Corning, NY) were seeded on a 22-mm^2 coverglass (Erie Scientific Co., Esco, Portsmouth, NH) and were grown for 48 h before transfection. Cells were transfected (3 h, 37 C) with either YFP empty vector or different YFP-IGFBP-3 constructs (300 ng DNA) using Lipofectamine Plus (Invitrogen) according to the manufacturer's instructions. In some imaging

experiments, cells were cotransfected with pCMX (empty vector) or pCMX-RXR-α (an expression vector containing human RXR-α cDNA; 300 ng DNA) and YFP or the indicated YFP-IGFBP-3 mutants (200 ng DNA). Cells were allowed to recover by incubation in medium containing 10% FBS for 24 h. For experiments in which cells were treated with RXR ligand, dialyzed FBS (GIBCO-Invitrogen) was used. The cells were washed with serum-free medium and treated with RXR-specific ligand (LG268) or vehicle for 24 h, the time previously used to show RXR ligand-dependent enhancement of nuclear localization in LAPC-4 prostate cancer cells (26). After recovery and treatment, the cells were fixed in 4% paraformaldehyde in 1x PBS (room temperature, 20 min). They were then washed twice with PBS at room temperature and permeabilized with 0.2% Triton X-100 in PBS (5 min on ice). The coverslips were mounted on slides using ProLong-Gold antifade

reagent containing 4',6-diamidino-2-phenylindole dihydrochloride (DAPI) to stain nuclear DNA (Molecular Probes-Invitrogen). RXR-α was detected using mouse monoclonal antibody to RXR-α and Alexa Fluor 594 goat antimouse IgG. Cells were imaged on a Carl Zeiss 510 Meta laser scanning confocal microscope (Carl Zeiss, Inc., Thornwood, NY) equipped with an Argon-LASER and x63 objective with numerical aperture (NA) 1.4. The subcellular distribution of YFP-WT-IGFBP-3 and YFP-MDGEA-IGFBP-3 seen by fluorescence imaging was previously validated using two methods of biochemical fractionation and immunoblotting (27) (unpublished results). In these experiments the fraction of YFP-MDGEA-IGFBP-3 in the nucleus was decreased by 75 ± 11% (SEM, n = 2) compared with YFP-WT-IGFBP-3.

GST-RXR pull down

Escherichia coli (MAX Efficiency DH5α Competent Cells; Invitrogen) were transformed with GST-RXR-α plasmid. The cells were grown overnight in LB broth (Quality Biological, Gaithersburg, MD) containing ampicillin (50 μg/ml). After centrifugation and rinsing with PBS, the cell pellet was resuspended in BugBuster Protein Extraction Reagent (Novagen-EMD, Darmstadt, Germany) containing protease inhibitors [(2-aminoethyl)-benzenesulfonyl fluoride hydrochloride, aprotinin, E-64, EDTA, and leupeptin; Calbiochem, San Diego, CA] and incubated on a rotating mixer at room temperature for 15 min. Glutathione-Sepharose 4B beads were added to the transformed *E. coli* lysate and to nontransformed *E. coli* lysate control mixed with GST, and incubated on a rotating mixer (1 h, room temperature).

After centrifugation, the beads were washed extensively and resuspended in Binding Buffer (Novagen).

Subconfluent PC-3 cells were transfected (3 h, 37 C) with different YFP-IGFBP-3 mutant plasmids using Lipofectamine Plus, and incubated in F12K medium containing 10% FBS for 24 h. The cells were washed with PBS and lysed in whole cell extract buffer [10 mM HEPES (pH 7.4), 10% glycerol, 250 mM NaCl, 1 mM EDTA, 0.1% Nonidet P-40, 1 mM dithiothreitol (DTT), and 1x protease inhibitor mixture] by rotating the plate at 4 C for 20 min. Cell lysates were transferred to tubes using a cell scraper (Sarstedt, Newton, NC). Cells were vortexed at high speed for 15 sec and placed in ice for another 5–10 min. After centrifugation (12,000 rpm, 5 min, 4 C), whole cell extracts (100 µg total protein) were incubated with 60 µl beads to which GST-RXR or GST had been

coupled (1 h, 4 C), the volume adjusted to 1.5 ml with 1x Binding Buffer, and the samples incubated on a rotating shaker overnight at 4 C. The beads were recovered by centrifugation, washed five times, resuspended in sodium dodecyl sulfate (SDS) protein gel solution (Quality Biological) containing 5% 2-mercaptoethanol, and the bound proteins eluted by boiling for 5 min.

The eluted proteins were analyzed by Western blotting. The samples were fractionated by electrophoresis using 4–20% SDS-PAGE (Bio-Rad Laboratories, Hercules, CA). The proteins were transferred onto nitrocellulose membranes, the membranes incubated with anti-GFP antibody and, after appropriate stripping, with anti-GST-HRP conjugate to confirm the presence of GST (results not shown) and anti-RAR antibodies. The presence of

bound antibody was detected using either SuperSignal West Pico or Femto Chemiluminescent Substrates kits (Pierce, Rockford, IL).

Coimmunoprecipitation

Subconfluent PC-3 cells were transfected with YFP-HBD-IGFBP-3 mutants and RXR-α, and cell lysates were prepared as previously described. Aliquots (300 μg total protein) of the whole cell extracts were precleared by incubation with 3 μg rabbit IgG (Sigma-Aldrich) plus 50 μl Protein A/G PLUS Agarose beads (Santa Cruz Biotechnology) for 1 h on a rotating shaker at 4 C. The volume was adjusted to 400 μl with incubation buffer [20 mM HEPES (pH 8.0), 150 mM KCl, 2.5 mM $MgCl_2$, 1 mM DTT, and 1× protease inhibitor mixture]. Equal aliquots of each precleared lysate were incubated with 5 μg rabbit RXR-α antibody (Santa Cruz Biotechnology) or control rabbit IgG. The volume was adjusted to

1 ml with incubation buffer and left overnight in a rotating shaker at 4 C. The next day, 50 µl Protein A/G Plus Agarose beads were added to the samples and incubated 1 h on a rotating shaker at 4 C. After centrifugation, the beads were washed with radioimmunoprecipitation assay buffer [150 mM NaCl, 1% NP-40, 0.5% sodium deoxycholate, 0.1% SDS, 50 mM Tris (pH 8.0), 1 mM DTT, and 1x protease inhibitor mixture], and subsequently four times (10 min each) with Buffer plus 1 M LiCl on a rotating shaker at 4 C. The beads were recovered by centrifugation, resuspended in SDS protein gel solution containing 5% 2-mercaptoethanol, and the bound proteins eluted by boiling for 5 min. The proteins were fractionated by electrophoresis using 7.5% SDS-PAGE, transferred onto nitrocellulose membranes, the membranes incubated with anti-GFP antibody, and, after appropriate stripping, with anti-RXR antibody (results not shown).

The presence of bound antibody was detected using SuperSignal West Pico Chemiluminescent Substrate.

Western blotting

Whole cell extracts were prepared from untransfected PC-3 cells or cells that had been transfected with pCMX-RXR-α as described previously. Protein concentrations were measured using the DC protein assay (Bio-Rad Laboratories). The proteins were fractionated using 7.5% SDS-PAGE under reducing conditions. After transfer of the fractionated proteins to nitrocellulose membranes, RXR-α was identified using mouse anti-RXR-α monoclonal antibody, followed by incubation with second antibody, and detected using SuperSignal West Pico Chemiluminescent Substrate.

Stimulation of RXRE promoter activity by RXR ligand

PC-3 or LNCaP cells were seeded in 24-well plates and transfected with 10 ng pCMX empty vector or pCMX-RXR-α expression vector plus 50 ng of the RXRE-luciferase reporter plasmid TK-CRBPII-Luc in serum-free medium. After 3 h, the incubation was continued in medium containing 10% dialyzed FBS for 24 h. The cells were washed twice and treated with 0.1 μM LG268 in serum-free medium for 24 h as indicated. Luciferase activity was measured in cell lysates using a dual luciferase reporter assay system (Promega, Madison, WI) and a Centro XS3 Microplate Luminometer LB 960 (Berthold Technologies, Oak Ridge, TN).

Apoptosis assay: Annexin V-APC staining analyzed by flow cytometry

To establish that IGFBP-3 induces cell death in prostate cancer

cells by an apoptotic process, we have followed the criteria of the Nomenclature Committee on Cell Death (54). Cell death was demonstrated by staining with Annexin V-APC and detected by flow cytometry. Annexin V binds to phospholipids located in the inner leaflet of the plasma membrane that are inaccessible in viable cells (55). Although they may become accessible early in apoptosis after translocation to the outer leaflet of the plasma membrane, in PC-3 cells Annexin V staining only occurs at later times after IGFBP-3 transfection, coincident with the appearance of staining by the vital dye 7-amino-actinomycin D, indicating loss of plasma membrane integrity (27). Thus, we consider Annexin V staining to be an indicator of loss of cell viability. To establish that IGFBP-3-induced cell death was due to an apoptotic process, we showed that Z-VAD-fmk, a broad-spectrum inhibitor of caspases, the cysteine-proteases responsible for cleaving specific targets to generate the

defining features of apoptosis, inhibited IGFBP-3-induction of Annexin V staining. The demonstration that inhibiting caspase activity inhibits cell death provides stronger evidence for a causal relationship than caspase activation alone (54).

PC-3 or LNCaP cells were grown to 70–80% confluence in six-well (35 mm) plates (Corning Inc., Costar) in F12K medium containing 10% FBS. The cells were rinsed twice with serum-free F12K medium and then transfected (37 C, 3 h) with 500 ng different YFP-IGFBP-3 plasmid constructs using Lipofectamine Plus. In these experiments, the concentration of YFP DNA used was reduced to make the percentage of transfected cells more comparable to that observed with YFP-IGFBP-3 constructs. The cells were allowed to recover by incubation at 37 C for 48 h in F12K medium containing 10% FBS, as previously described (27)

unless otherwise specified. In other experiments, untransfected PC-3 or LNCaP cells were starved by incubation in serum-free medium for 24 h, before being treated with 0.1 μM LG268 or dimethylsulfoxide (DMSO) vehicle in serum-free medium for 48 h.

For analysis of apoptosis, attached cells were trypsinized, combined with cells floating in the media, and centrifuged (1200 rpm, 5 min). The cell pellets were washed twice with PBS and resuspended in 1x binding buffer [BD Biosciences-Pharmingen; 10 mM HEPES (pH 7.4), 140 mM NaCl, and 2.5 mM $CaCl_2$]. The cells were stained using 500 μl binding buffer containing 5 μl Annexin V-APC at room temperature in the dark for 20 min. Cells were analyzed using a FACSCalibur cytofluorometer (BD Biosciences-Pharmingen) and Summit software (DakoCytomation, Fort Collins, CO) as previously described.

In addition to undergoing apoptosis, cells transfected with YFP-IGFBP-3 constructs also undergo proteolytic degradation of the fusion proteins (27). For this reason, we have not performed parallel immunoblots on the transfected cells to attempt to quantify the relative level of expression of the various YFP-IGFBP-3 fusion proteins.

RESULTS

COOH-terminal IGFBP-3 mutants differentially affect nuclear localization and binding to RXR-α

Residues 215–232 near the COOH terminus of IGFBP-3 (Fig. 1A) are highly enriched in basic amino acids, and contain a bipartite NLS (22, 56), a HBD (2, 57), and binding sites for RXR-α (26) and other proteins (2, 58).[2] The distal basic cluster in the bipartite NLS, residues 228-KGRKR-232, is required for the translocation of IGFBP-3 to the nucleus. Changing residues 228–232 to the

[2] The bipartite NLS consists of 215-KK-216, an 11-amino acid spacer that includes 220-KKK-222, and 228-KGRKR-232 (22, 56). Residues 219–226 satisfy the requirements for a consensus HBD, X-BBB-XX-B-X, where B is a basic amino acid, and X is usually a hydropathic amino acid (57, 64, 65). For convenience, we refer to the entire 215–232 region as the HBD.

corresponding sequence in IGFBP-1, MDGEA, in a YFP-IGFBP-3 fusion protein prevented the YFP-MDGEA-IGFBP-3 mutant from being concentrated in the nucleus (27). Similar results had been observed when digitonin-permeabilized Chinese hamster ovary cells were incubated with MDGEA-IGFBP-3 protein *in vitro*, as well as after expression of a fusion protein in which an IGFBP-3 peptide (amino acids 215–232) containing the MDGEA substitution was fused to EGFP (25).

To determine whether 228-KGRKR-232 is the only domain in the 215–232 region that is involved in the nuclear localization of full-length IGFBP-3, we used confocal imaging to examine the subcellular distribution of a series of YFP-IGFBP-3 fusion proteins in which different groups of the 11 residues that differ between IGFBP-3 and IGFBP-1 were mutated to the IGFBP-1 sequence

(Fig. 1). The nuclear-cytoplasmic distribution observed by fluorescence imaging corresponded to that determined using two methods of biochemical fractionation, followed by immunoblotting (27) (unpublished results).

Residues 228-KGRKR-232 in the NLS were replaced by MDGEA in three IGFBP-3 variants: YFP-MDGEA-IGFBP-3, YFP-HBD-9m-IGFBP-3, and YFP-HBD-11m-IGFBP-3. All three mutants localized predominantly to the cytoplasm. Interestingly, a fourth IGFBP-3 variant, HBD-6m-IGFBP-3, also localized predominantly in the cytoplasm, even though it retained the WT 228-KGRKR-232 sequence. This suggests that in addition to 228-KGRKR-232, some or all of the residues that were substituted in HBD-6m-IGFBP-3 (K216-K220-K221-K222-R225-P226) also contribute to the nuclear localization of IGFBP-3.

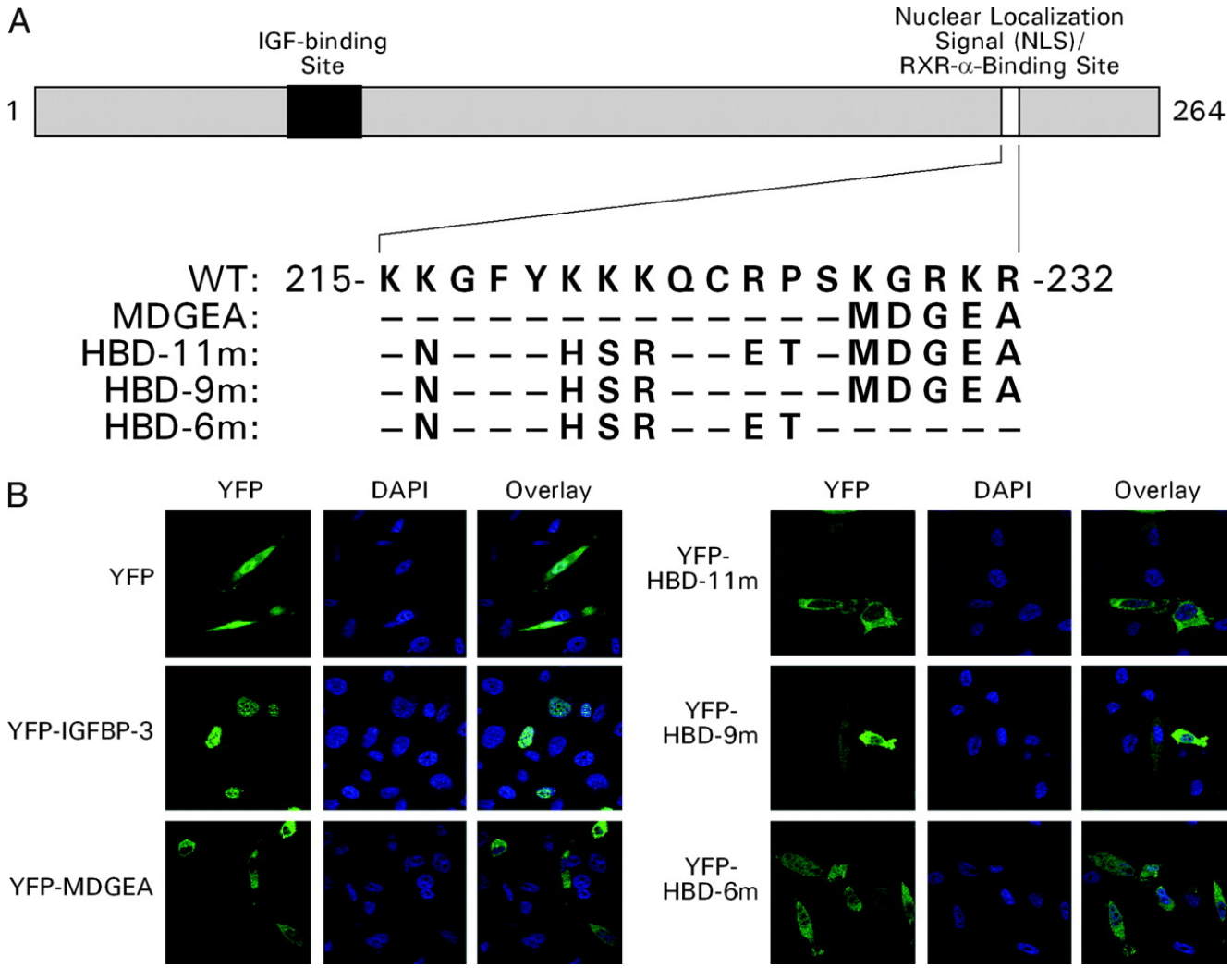

FIG. 1. A, Schematic diagram showing the IGFBP-3 mutants used. A COOH-terminal basic region of IGFBP-3 (residues 215–232) contains the NLS [residues 228-KGRKR-232 (25)] and confers the ability to bind RXR-α (26). Of the 18 amino acids in the region, 11 differ from the corresponding sequence of IGFBP-1. They are indicated in the HBD-11m-IGFBP-3 mutant; identical amino acids are indicated by a *dash*. We also examined mutants with partial substitutions of these residues (MDGEA-IGFBP-3, HBD-9m-IGFBP-3, and HBD-6m-IGFBP-3). In some experiments the NH_2-terminal IGF-binding site (*black portion of the bar*) also was mutated in HBD-11m-IGFBP-3 by substituting alanine for six critical amino acids [^{56}I, ^{57}Y, ^{75}R, ^{77}L, ^{80}L, and ^{81}L (5)]. B, Confocal imaging of PC-3 cells transfected with WT and mutant YFP-IGFBP-3 constructs. PC-3 cells were transfected with YFP empty vector (YFP) or the indicated YFP-IGFBP-3 constructs: YFP-WT IGFBP-3 (YFP-IGFBP-3), YFP-MDGEA-IGFBP-3, YFP-HBD-11m-IGFBP-3, YFP-HBD-9m-IGFBP-3, and YFP-HBD-6m-IGFBP-3. The cells were fixed, incubated with the nuclear stain DAPI, and examined by confocal imaging. Images from representative fields show *green* fluorescence (YFP) (*left column*), *blue* fluorescence (DAPI) (*center column*), and overlay of DAPI and YFP fluorescence (*right column*).

The ability of the different IGFBP-3 mutants to bind RXR-α was examined by GST pull-down experiments (Fig. 2). Lysates were prepared from PC-3 cells that had been transfected with plasmids expressing YFP or different YFP-IGFBP-3 fusion proteins, and were incubated with Glutathione-Sepharose beads to which GST-RXR-α or GST control were coupled. Proteins that bound to the beads were eluted and identified by SDS-PAGE using antibodies to GFP. YFP-WT-IGFBP-3 and three of the YFP-IGFBP-3 variants (YFP-MDGEA-IGFBP-3, YFP-HBD-6m-IGFBP-3, and YFP-HBD-9m-IGFBP-3) bound to GST-RXR-α, but not to the GST control (Fig. 2A, *left-upper panel*), indicating that they bound specifically to RXR-α. By contrast, YFP-HBD-11m-IGFBP-3, like the YFP control, was the only IGFBP-3 mutant that did not bind to GST-RXR-α (Fig. 2A, *left-upper panel*), even though both proteins

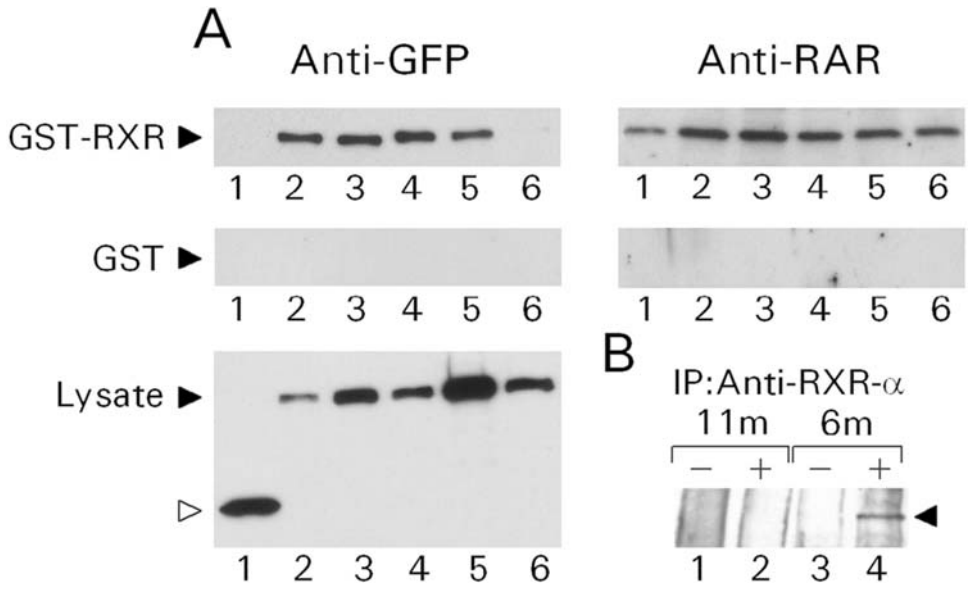

FIG. 2. Binding of YFP-IGFBP-3 mutant proteins to RXR-α. A, *In vitro* binding of YFP-IGFBP-3 mutant proteins to GST-RXR-α fusion proteins. GST-RXR-α (expressed in *E. coli*) or GST control was coupled to Glutathione-Sepharose-4B beads. PC-3 cells were transfected with YFP empty vector (lane 1), YFP-WT-IGFBP-3 (lane 2), YFP-MDGEA-IGFBP-3 (lane 3), YFP-HBD-6m-IGFBP-3 (lane 4), YFP-HBD-9m-IGFBP-3 (lane 5), and YFP-HBD-11m-IGFBP-3 (lane 6). After 24 h, total cell lysates were prepared and incubated overnight at 4 C with beads that had been coupled with GST-RXR or GST. Bound proteins were eluted and examined by Western blotting using antibodies to GFP, which recognize YFP (*upper-left panel*). Similar results were obtained in two other experiments. *Lower-left panel*, Lysates used for the GST pull down were blotted with anti-GFP. Anti-GFP binds to approximately 27-kDa YFP (*open arrowhead*, lane 1) and to the YFP moiety of the approximately 67-kDa YFP-IGFBP-3 fusion proteins (*solid arrowheads, upper* and *lower-left panels*). For clarity, lanes separating the individual lanes shown have been deleted. Lanes 1–3 and lanes 4–6 were taken from different gels. The greater intensity of the YFP-HBD-9m-IGFBP-3 lysate signal relative to the YFP-HBD-11m-IGFBP-3 lysate in this immunoblot is not consistently observed, and does not account for the inability to detect YFP-HBD-11m-IGFBP-3 by GST-RXR pull down. As an additional control, the GST-RXR and GST pull-down blots were stripped and immunoblotted with anti-RAR (*upper-right panel*). Endogenous RAR, a known partner of RXR, binds specifically to GST-RXR in all lysates, excluding the possibility that the inability of YFP-HBD-11m-IGFBP-3 to bind to GST-RXR was due to nonspecific inhibitors or competitors of binding to RXR-α in the cell lysates. It has been reported that IGFBP-3 can dissociate preformed RXR:RAR heterodimers (by binding to either RXR or RAR) (29). Decreased binding of RAR to GST-RXR, however, would not be expected in our experiment because of the large excess of GST-RXR. B, Coimmunoprecipitation of YFP-IGFBP-3 mutants and RXR-α from PC-3 cell lysates. PC-3 cells were transfected with pCMX-RXR-α expression vector and either YFP-HBD-11m-IGFBP-3 (lanes 1 and 2) or YFP-HBD-6m-IGFBP-3 (lanes 3 and 4). After 24 h, cell lysates were prepared, precleared, and equal aliquots were incubated with rabbit IgG control (–, lanes 1 and 3) or with antibody to RXR-α (+, lanes 2 and 4). After 16 h, Protein A/G Plus Agarose beads were added to all the samples. After high-stringency washes, the immunoprecipitated proteins were eluted and analyzed by Western blotting using antibody to GFP to identify the YFP-IGFBP-3 mutant proteins. The position of immunoreactive YFP-IGFBP-3 is indicated by a *solid arrowhead*. The lanes shown are from the same gel. Lanes separating lanes 1 and 2 from lanes 3 and 4 have been removed for clarity of presentation, and the images spliced to put them in closer proximity.

were abundant in the cell lysates that had been incubated with the GST-RXR beads (Fig. 2A, *left-lower panel*). GST-RXR-α did bind to endogenous RAR, a known binding partner of RXR, in all cell lysates examined, including those from cells expressing YFP-HBD-11m-IGFBP-3 (Fig. 2A, *right-upper panel*). This important control demonstrates that the total cell lysates do not contain nonspecific inhibitors of binding to GST-RXR-α, or appreciable amounts of soluble proteins that might compete for binding to RXR-α. We conclude from these results that the entire 215–232 region of IGFBP-3 must be mutated to the IGFBP-1 sequence to abolish binding to RXR.

Our results support and extend those obtained by Liu *et al*. (26) using recombinant IGFBP-3 mutant proteins expressed in *E. coli*. They showed that an IGFBP-3 NLS mutant protein in which

residues 228 and 230 were substituted, 228-eGgKR-232,[3] bound to GST-RXR-α, whereas HBD-11m-IGFBP-3 protein expressed in baculovirus did not. Recently, however, Schedlich *et al*. (59) reported that the 228-MDGEA-232 mutation by itself greatly decreased binding to GST-RXR-α. The reason for the difference between their results using purified MDGEA-IGFBP-3 protein, and our results using lysates from cells expressing the MDGEA mutant or those of Liu *et al*. (26) using a similar mutant protein, 228-eGgKR-232, remains to be elucidated.

Schedlich *et al*. (59) also reported that mutation of a second COOH-terminal site in IGFBP-3, 220-KKK-222, reduced binding

[3] The sequence of the NLS mutant (228-eGgKR-232) inadvertently was published incorrectly (26) as 228-eGcKR-232 (Mascarenhas, D., Rechler, MM.).

to GST-RXR-α. These residues, however, also are mutated in the HBD-6m-IGFBP-3 and HBD-9m-IGFBP-3 mutants that we found could bind to GST-RXR-α (Fig. 2A). Because WT IGFBP-3 and RXR-α coimmunoprecipitated from HeLa cell nuclear extracts (26), we examined the ability of HBD-6m-IGFBP-3 to bind to RXR-α in living cells by coimmunoprecipitation of extracts from PC-3 cells expressing both proteins (Fig. 2B). Anti-RXR-α specifically immunoprecipitated YFP-HBD-6m-IGFBP-3 (lane 4) but not YFP-HBD-11m-IGFBP-3 (lane 2) from lysates of transfected PC-3 cells. Neither mutant fusion protein was immunoprecipitated by control IgG (lanes 1 and 3). These results support our conclusion from the GST pull-down experiments that all 11 amino acids in the 215–232 region of IGFBP-3 that differ from IGFBP-1 must be mutated to the IGFBP-1 sequence to abolish binding to RXR *in vitro* as well as in living cells. Under our

experimental conditions, IGFBP-3 mutants in which the 228-KGRKR-232 or 220-KKK-222 sites were mutated still bind RXR-α, even though they do not translocate to the nucleus.

Nuclear RXR-α does not transport cytoplasmic IGFBP-3 NLS mutants that bind RXR-α to the nucleus of PC-3 cells even after incubation with RXR ligand

Endogenous RXR-α and IGFBP-3 localized more completely to the nucleus when LAPC-4 human prostate cancer cells were incubated with a synthetic RXR-selective ligand, LG1069 (26). These observations led to the suggestion that RXR-α activated by RXR ligand could bind to IGFBP-3 and transport it to the nucleus. Our identification of several IGFBP-3 NLS mutants that localized to the cytoplasm but still were able to bind RXR-α (Figs. 1 and 2) enabled

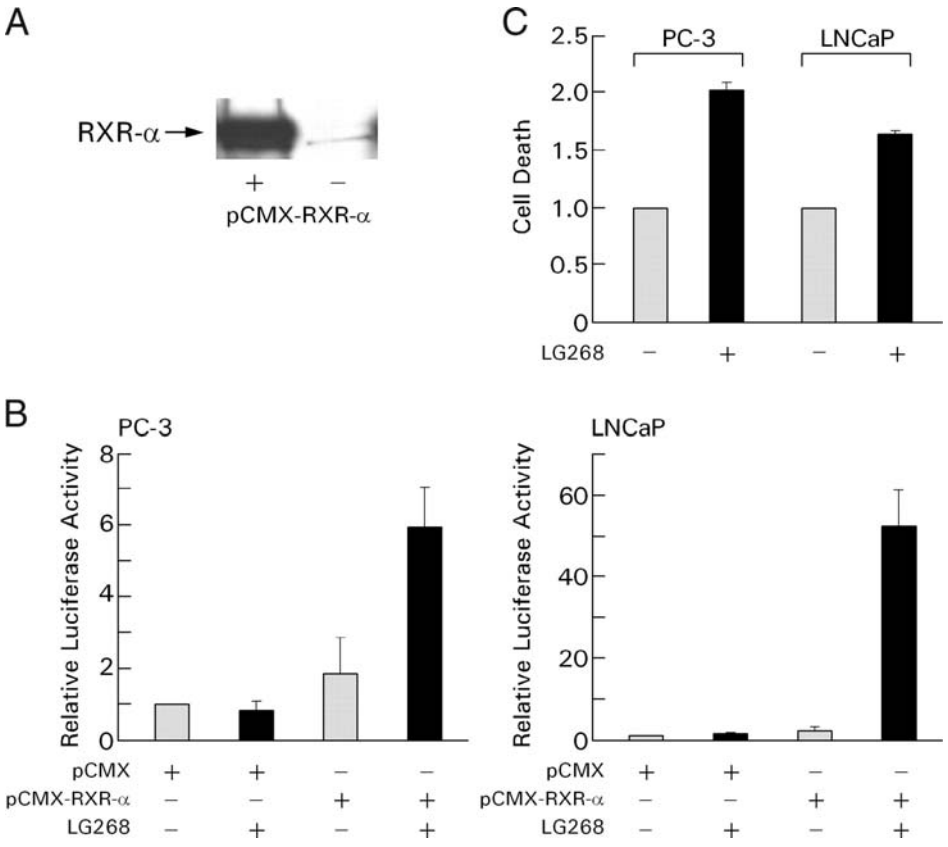

FIG. 3. The RXR ligand LG268 activates endogenous RXR-α, and induces apoptosis in PC-3 and LNCaP human prostate cancer cell lines. A, Immunoblot of PC-3 cell lysates with anti-RXR-α antibody. Cells in the *left lane* (+) were transfected with pCMX-RXR-α expression vector. Cells in the *right lane* (–) were not transfected. The *arrow on the left* shows the migration of recombinant human RXR-α standard. B, RXRE luciferase assay. PC-3 cells (*left*) or LNCaP cells (*right*) were transfected with pCMX or pCMX-RXR-α as indicated, and an RXRE-luciferase reporter plasmid (TK-CRBPII-Luc) for 3 h. After incubation in medium containing 10% charcoal-treated FBS for 24 h, the cells were washed and then incubated in serum-free medium for an additional 24 h with LG268 (0.1 μM) or DMSO vehicle. Luciferase activity is expressed relative to control cells incubated with DMSO. The mean ± SE of three experiments is plotted. In these experiments, 0.1 μM LG268 stimulated luciferase activity 21-fold in LNCaP cells and 5-fold in PC-3 cells that had been transfected with pCMX-RXR-α. In other experiments 1 μM LG268 stimulated luciferase activity in PC-3 cells to the same extent as 0.1 μM LG268-treated LNCaP cells (results not shown). C, LG268 induces apoptosis in untransfected PC-3 and LNCaP cells. PC-3 cells (*two left lanes*) and LNCaP cells (*two right lanes*) were incubated for 48 h in serum-free medium with (+, *black bars*) or without (–, *gray bars*) 0.1 μM LG268. Cell death was determined by Annexin V staining and flow cytometry, and is expressed relative to control cells treated with vehicle for each cell line. The mean ± SE for three experiments is plotted. $P = 0.05$ for PC-3 cells and $P = 0.06$ for LNCaP cells using the Student's t test. The ability of LG268 to induce apoptosis but not RXRE-dependent promoter activity (B) in nontransfected PC-3 and LNCaP cells may reflect differences in the experimental conditions, or may indicate that RXR can induce apoptosis by mechanisms that do not involve transcription (63).

us to test directly whether ligand-activated RXR-α could transport IGFBP-3 to the nucleus in PC-3 cells.

To determine the effect of RXR ligand on the nuclear localization of YFP-IGFBP-3 fusion proteins in PC-3 cells by confocal imaging, we transfected cells with the pCMX-RXR-α expression vector to overcome the low abundance of endogenous RXR-α (Fig. 3A). The RXR ligand, LG268 (46), a potent, highly selective derivative of LG1069, stimulated RXRE-dependent promoter activity in PC-3 cells that had been transfected with pCMX-RXR-α (Fig. 3B, *left panel*). Similar results were obtained using LNCaP human prostate cancer cells (Fig. 3B, *right panel*) that express similar levels of endogenous RXR-α (60).

Confocal imaging was performed on PC-3 cells that had been transfected with pCMX-RXR-α to ensure that sufficient RXR-α

was present in the nucleus to serve potentially as a chaperone to deliver cytoplasmic IGFBP-3 to the nucleus (Fig. 4). Both RXR-α and YFP-WT-IGFBP-3 were localized mainly in the nucleus, and incubation with LG268 did not affect their distribution. Even though transfected RXR-α was predominantly nuclear, the three coexpressed IGFBP-3 mutants that contained the 228-MDGEA-232 NLS mutation but could bind to RXR-α (*i.e*. MDGEA, HBD-9m, and HBD-6m) did not translocate to the nucleus, even after incubation with LG268. Although these mutants can bind RXR-α, they remain in the cytoplasm despite overexpression of RXR-α and its activation by RXR ligand. As expected, LG268 did not affect the cytoplasmic localization of HBD-11m-IGFBP-3 because this IGFBP-3 mutant does not bind RXR-α. These results demonstrate that RXR-α is unable to transport cytoplasmic IGFBP-3 mutants to the nucleus in PC-3 cells.

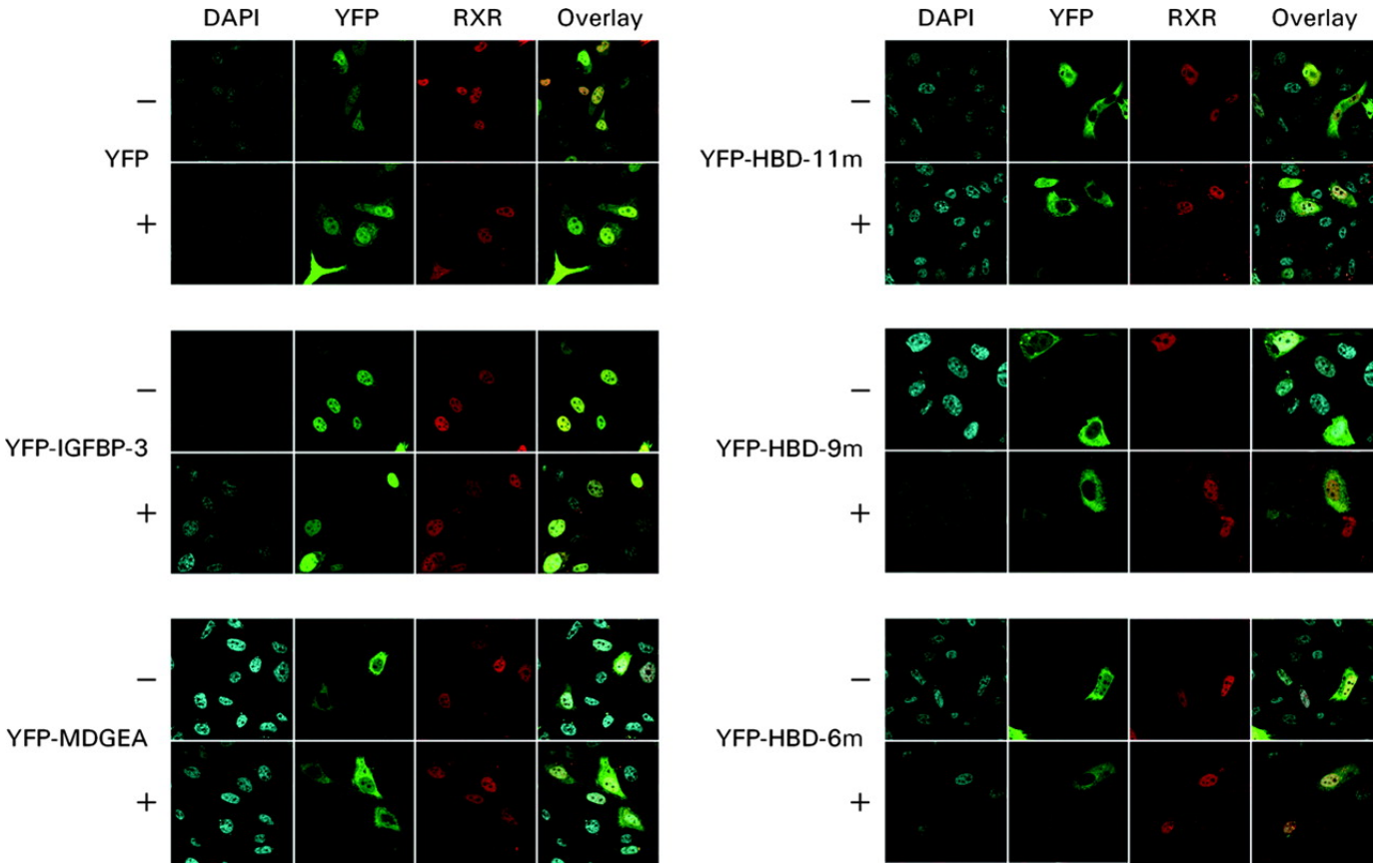

FIG. 4. Treatment of PC-3 cells with RXR ligand does not change the subcellular localization of expressed IGFBP-3 constructs and RXR-α. PC-3 cells were cotransfected for 3 h with pCMX-RXR-α and either YFP empty vector (YFP), YFP-WT IGFBP-3 (YFP-IGFBP-3), or the indicated YFP-IGFBP-3 mutants (YFP-MDGEA, YFP-HBD-11m, YFP-HBD-9m, YFP-HBD-6m). After 24 h incubation in medium containing 10% dialyzed FBS, the cells were washed and incubated in serum-free medium without ("–") or with ("+") 1 μM of the RXR-specific ligand, LG268, for 24 h. The cells were then stained with DAPI, fixed, incubated with mouse anti-RXR monoclonal antibody/Alexa Fluor 594 goat antimouse IgG, and examined by confocal microscopy. From *left to right*, the *columns* show *blue* fluorescence (DAPI), *green* fluorescence (YFP), *red* fluorescence (RXR-α), and an overlay.

YFP-HBD-11m-IGFBP-3 can induce apoptosis in prostate cancer cells although it does not bind RXR-α

Exogenous IGFBP-3 (5) or nonsecreted, transfected IGFBP-3 (27) can induce cell death in PC-3 cells by apoptosis (54). Before examining whether HBD-11m-IGFBP-3, the IGFBP-3 mutant that does not bind RXR-α, was able to induce apoptosis in PC-3 cells, we wanted to establish that the levels of endogenous RXR-α were sufficient to induce apoptosis in PC-3 cells as previously reported in LNCaP prostate cancer cells (26) that express endogenous RXR-α at a similar low level (60).

PC-3 and LNCaP cells were incubated with LG268 for 48 h, after which cell death was determined by Annexin V-APC staining followed by flow cytometry (Fig. 3C). Annexin V binding to phospholipids in the inner leaflet of the plasma membrane reflects

loss of cell viability (27, 55). Cell death was significantly increased by the RXR ligand in PC-3 cells (2.03 ± 0.29-fold, mean ± SE, n = 3; $P = 0.05$), and to a similar extent in LNCaP cells (1.66 ± 0.03-fold, mean ± SE, n = 3; $P = 0.06$). These results indicate that PC-3 cells, like LNCaP cells, express sufficient RXR to induce apoptosis.

The ability of different YFP-IGFBP-3 mutants to induce apoptosis in PC-3 cells was examined (Fig. 5A). Both YFP-WT-IGFBP-3 and YFP-MDGEA-IGFBP-3, which is not concentrated in the nucleus, induced cell death as previously reported (27). YFP-HBD-11m-IGFBP-3, which does not bind RXR-α and is not concentrated in the nucleus, also increased Annexin V staining, indicating that direct binding of IGFBP-3 to RXR-α (Fig. 2A) is not necessary for IGFBP-3 to induce cell death. Annexin V staining induced by all of

the fusion proteins was inhibited by the broad-spectrum caspase inhibitor, Z-VAD-fmk, indicating that cell death resulted from apoptosis (54). WT YFP-IGFBP-3 and YFP-HBD-11m-IGFBP-3 also induced cell death in LNCaP cells to similar extents [1.81 ± 0.29-fold and 1.65 ± 0.13-fold (mean ± SE, n = 2), respectively] (Fig. 5B).

To determine whether the induction of apoptosis by YFP-HBD-11m-IGFBP-3 in PC-3 cells was IGF independent, a second set of six mutations (6m) was introduced into the IGF-binding site (see legend to Fig. 1). Apoptosis was induced by the double mutant, YFP-6m/HBD-11m-IGFBP-3, indicating that binding to IGFs was not involved (Fig. 5A). Thus, IGFBP-3 does not need to bind to either IGF-I/IGF-II or RXR-α to be able to induce apoptosis in PC-3 cells.

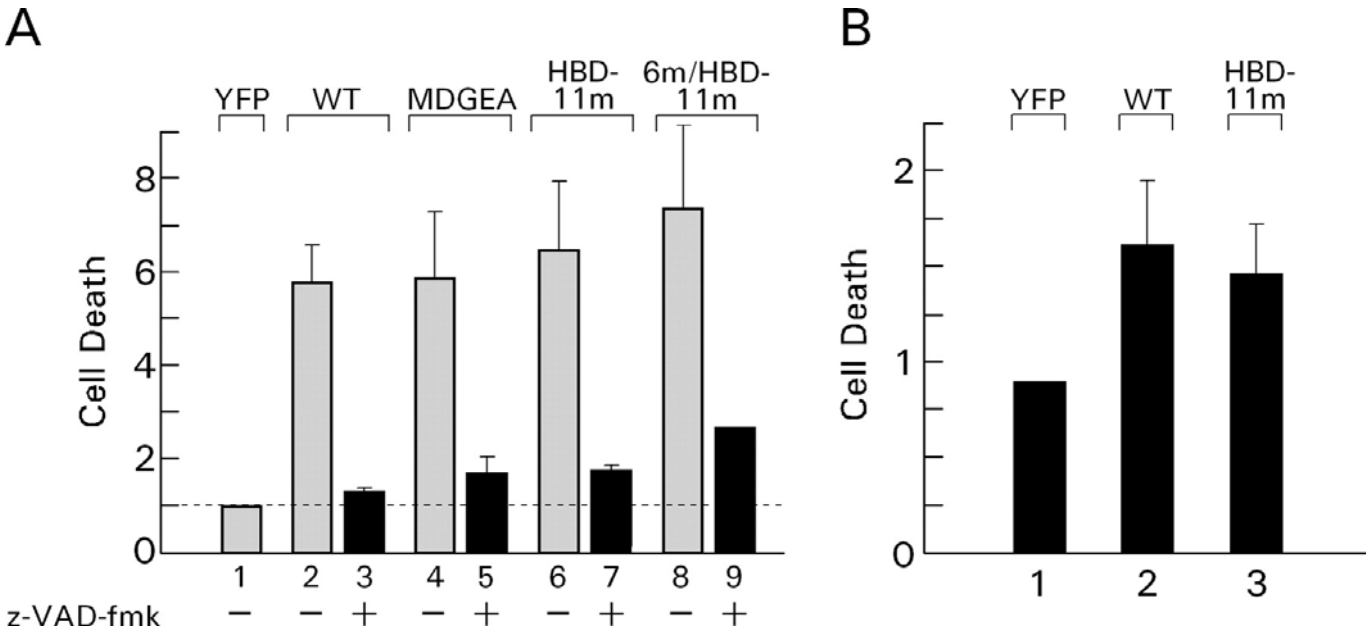

FIG. 5. YFP-HBD-11m-IGFBP-3 induces apoptosis in PC-3 and LNCaP human prostate cancer cells. A, PC-3 cells were transfected with YFP empty vector (*lane 1*), YFP-WT-IGFBP-3 (*lanes 2* and *3*), YFP-MDGEA-IGFBP-3 (*lanes 4* and *5*), YFP-HBD-11m-IGFBP-3 (*lanes 6* and *7*), and YFP-6m/HBD-11m-IGFBP-3 (*lanes 8* and *9*) for 3 h, then incubated in serum-containing medium in the presence (+) or absence (–) of the general caspase inhibitor, Z-VAD-fmk (20 μM). Cell death was determined by Annexin V staining, which was quantified using flow cytometry, and is expressed relative to YFP-empty vector in the same experiment (*dashed line*). The mean ± SE of three experiments is plotted. B, YFP-HBD-11m-IGFBP-3 induces cell death in LNCaP cells. LNCaP cells were transfected with YFP, YFP-WT-IGFBP-3, or YFP-HBD-11m-IGFBP-3 for 3 h, and allowed to recover by incubation in DMEM:F12K medium containing 5% FBS for 24 h. After incubation for another 48 h in serum-free medium, cell death was determined by Annexin V staining and flow cytometry as described previously. The mean ± SE is plotted for two experiments.

DISCUSSION

IGFBP-3 can induce apoptosis in human prostate cancer cells independently of binding and sequestering IGFs, but the mechanisms are not well understood. It is a secreted protein that can be internalized (20), translocate to the nucleus (23-27), and bind to the nuclear retinoid receptor RXR-α (26, 29). RXR ligand promoted the colocalization of IGFBP-3 and RXR-α to the nucleus, and IGFBP-3 induced apoptosis in a murine embryonal carcinoma cell line only if the cells expressed the nuclear retinoid receptor RXR-α (26). These observations raised the possibility that direct binding of IGFBP-3 to RXR-α may be required for both activities. To test this hypothesis, in the present study, we have generated mutants in a COOH-terminal region of IGFBP-3 that contains both the NLS and the RXR binding site. We show that IGFBP-3 variants in which the NLS is mutated but that still can bind RXR-α are not

cotransported to the nucleus of cells in which RXR-α is overexpressed, even in the presence of RXR ligand. We also show that an IGFBP-3 variant that does not bind RXR-α is able to induce apoptosis in PC-3 human prostate cancer cells in an IGF-independent manner.

Residues 215–232 near the COOH terminus of IGFBP-3 are highly enriched in basic amino acids, and contain a bipartite NLS (22) and a binding site for RXR-α (26). Unlike IGFBP-3, IGFBP-1, a related member of the IGFBP family, does not localize to the nucleus (24) or bind RXR-α (26). The primary IGFBP-3 sequence in this region differs from the corresponding sequence of IGFBP-1 at 11 of the 18 amino acids. We have systematically replaced different combinations of these 11 amino acids with the corresponding IGFBP-1 sequence to define better the requirements for RXR-α

binding and nuclear localization (Fig. 1). Substitution of all 11 amino acids to make the sequence of IGFBP-3 residues 215–232 identical to the corresponding sequence of IGFBP-1 (HBD-11m-IGFBP-3) abolished the ability of the IGFBP-3 mutant to bind RXR-α as previously reported (26). Mutation of five amino acids at the COOH-terminal end of this sequence, 228-KGRKR-232, that are part of the bipartite NLS (22), to MDGEA, the corresponding sequence in IGFBP-1, abolished nuclear translocation (Refs. 25 and 27 , and the present studies). In addition, we mutated the six amino acids besides 228-KGRKR-232 that differ in IGFBP-1 (K216-K220-K221-K222-R225-P226) to the IGFBP-1 sequence (HBD-6m-IGFBP-3), and four of these residues (K216-K220-K221-K222) in combination with the MDGEA mutation (HBD-9m-IGFBP-3). In GST pull-down experiments, WT IGFBP-3 in PC-3 cell lysates bound to GST-RXR-α but not to GST as reported with purified

protein (26, 29). Three of the IGFBP-3 mutants (MDGEA-IGFBP-3, HBD-6m-IGFBP-3, and HBD-9m-IGFBP-3) also bound to GST-RXR-α. Only HBD-11m-IGFBP-3 in which all 11 sites had been mutated to the IGFBP-1 sequence did not bind to GST-RXR-α. The same binding specificity was observed in living cells. Recombinant WT IGFBP-3 coimmunoprecipitated with endogenous RXR-α from HeLa cell nuclear extracts (26). In lysates from PC-3 cells transfected with RXR-α expression plasmids, cotransfected YFP-HBD-6m-IGFBP-3 but not YFP-HBD-11m-IGFBP-3 was immunoprecipitated by antibody to RXR-α (Fig. 2B). It is unlikely that substitution of two additional sites in HBD-11m-IGFBP-3 compared with HBD-9m-IGFBP-3, R225E-P226T accounts for the loss of RXR-α binding because HBD-6m-IGFBP-3 contains the same substitution, yet is able to bind to RXR-α in both GST pull-down and coimmunoprecipitation experiments (Fig. 2). Our results

indicate that residues throughout the entire 215–232 region of IGFBP-3 are necessary for RXR-α binding and that binding to RXR-α is not lost until the entire 215–232 region is converted to the IGFBP-1 sequence.

In contrast to our results, Schedlich *et al*. (59) recently reported that IGFBP-3 mutant proteins containing either the MDGEA mutation or the substitution of HSR for 220-KKK-222 could not bind to GST-RXR-α. The 220-HSR-222 mutation is present in HBD-6m-IGFBP-3, which we find binds to RXR-α in GST pull-down and coimmunoprecipitation experiments. The different results may be due to the different samples used, purified mutant IGFBP-3 proteins (59) or lysates from cells expressing the mutant proteins. It remains to be determined which experimental system is more physiologically relevant. For example, other factors present in the

cell lysates may enable MDGEA-IGFBP-3 and HBD-6m-IGFBP-3 to bind to RXR-α.

As expected, the three IGFBP-3 variants in which 228-KGRKR-232 was replaced by MDGEA (MDGEA-IGFBP-3, HBD-9m-IGFBP-3, and HBD-11m-IGFBP-3) were predominantly located in the cytoplasm. Unexpectedly, HBD-6m-IGFBP-3 (in which only residues K216-K220-K221-K222-R225-P226 were mutated) also was predominantly localized to the cytoplasm in all of the fluorescing PC-3 cells we examined, even though the native 228-KGRKR-232 sequence was intact. This indicates that residues 228-KGRKR-232 at the COOH-terminal end of the bipartite NLS are necessary but not sufficient to ensure nuclear localization.

Incubation of LAPC-4 human prostate cancer cells with RXR ligand caused both IGFBP-3 and RXR-α to localize more

completely to the nucleus, suggesting that ligand-activated RXR-α might transport IGFBP-3 to the nucleus (26). Expressed RXR-α and YFP-WT-IGFBP-3 also localized predominantly to the nucleus in PC-3 cells. Together with the availability of cytoplasmic IGFBP-3 NLS mutants that can bind RXR-α, the nuclear localization of transfected RXR-α made it possible to test directly whether RXR-α could transport the IGFBP-3 mutants to the nucleus. The VDR was able to deliver RXR-α, its heterodimer partner, to the nucleus after incubation with 1,25-dihydroxyvitamin D (42, 43). Schedlich *et al*. (59) discussed the possibility that cytoplasmic IGFBP-3:RXR-α complexes may bind to importin-β through the RXR-α nuclear localization sequence, enabling cotransport to the nucleus. However, in our case, despite transfection of PC-3 cells with RXR-α and their subsequent treatment with RXR ligand, the three cytoplasmic IGFBP-3 NLS mutants (MDGEA-IGFBP-3, HBD-6m-

IGFBP-3, and HBD-9m-IGFBP-3) did not translocate to the nucleus, even though they were able to bind to RXR-α.

Both PC-3 and LNCaP human prostate cancer cell lines contain low (60) but functionally significant levels of RXR-α, as indicated by the ability of RXR ligand to induce cell death (Fig. 3C). Transfection of PC-3 or LNCaP cells with the RXR-α-nonbinding mutant, YFP-HBD-11m-IGFBP-3, caused a loss of cell viability as reflected by increased Annexin V staining. Incubation of PC-3 cells with the broad-spectrum caspase inhibitor, Z-VAD-fmk, inhibited the increase in cell death, indicating that the decrease in cell viability was triggered by apoptosis. Moreover, concurrent mutation of the NH_2-terminal IGF-binding site in HBD-11m-IGFBP-3 did not affect its ability to induce apoptosis in PC-3 cells, indicating that it acted in an IGF-independent manner as previously

shown for WT IGFBP-3 (5, 27). These results indicate that IGFBP-3 can induce apoptosis in prostate cancer cell lines without binding either IGFs or RXR-α. Even if MDGEA-IGFBP-3 does not bind to RXR-α as recently reported by Schedlich *et al*. (59) in contrast to our results, their result would still support our main conclusion that IGFBP-3 does not need to bind to RXR-α to induce apoptosis in prostate cancer cells because MDGEA-IGFBP-3 induces apoptosis in PC-3 cells (Ref. 27 and present results). WT IGFBP-3, but not HBD-11m-IGFBP-3, induced the inhibition of vascular endothelial-derived growth factor-stimulated proliferation and survival in human umbilical vein endothelial cells in an IGF-I receptor-independent manner, but it is not known whether RXR-α is involved in this activity (61).

In summary, IGFBP-3 binds to RXR-α, and expression of RXR-α (26) or addition of RXR ligand (26, 62) is required for the induction of apoptosis by IGFBP-3 in some experimental systems. The present study demonstrates that IGFBP-3 can induce apoptosis in PC-3 and LNCaP human prostate cancer cells without binding to RXR-α. Synergy between the two pathways still may occur without direct binding of the two proteins, *e.g.* by interaction of IGFBP-3 with protein products of genes that are downstream from RXR-α or heterodimer nuclear receptor partners of RXR-α (29, 30), or by stimulation of IGFBP-3 signaling pathways (16, 63) to activate pro-apoptotic pathways.

ACKNOWLEDGMENTS.

I express sincere gratitude to Prof. Massimo Federici and Prof. Fabrizio Barbetti and gratefully thank Dr. Matt Rechler.

Abbreviations

DAPI, 4',6-Diamidino-2-phenylindole dihydrochloride; DMSO, dimethylsulfoxide; DTT, dithiothreitol; FBS, fetal bovine serum; fmk, fluoromethylketone; GFP, green fluorescent protein; GST, glutathione S-transferase; HBD, heparin binding domain; HRP, horseradish peroxidase; IGFBP, IGF binding protein; NLS, nuclear localization signal; RAR, retinoic acid receptor; RXR, retinoid X receptor; RXRE, retinoid X receptor response element; SDS, sodium dodecyl sulfate; TK-CRBPII-Luc, thymidine kinase promoter-cellular retinol binding protein II RXRE-luciferase; VDR, vitamin D receptor; WT, wild type; YFP, yellow fluorescent protein; Z, benzyloxycarbonyl.

REFERENCES

1. **Rechler MM, Clemmons DR** 1998 Regulatory actions of insulin-like growth factor-binding proteins. Trends Endocrinol Metab 9:176–183

2. **Firth SM, Baxter RC** 2002 Cellular actions of the insulin-like growth factor binding proteins. Endocr Rev 23:824–854

3. **Imai Y, Moralez A, Andag U, Clarke JB, Busby Jr WH, Clemmons DR** 2000 Substitutions for hydrophobic amino acids in the N-terminal domains of IGFBP-3 and -5 markedly reduce IGF-I binding and alter their biologic actions. J Biol Chem 275:18188–18194

4. **Buckway CK, Wilson EM, Ahlsen M, Bang P, Oh Y, Rosenfeld RG** 2001 Mutation of three critical amino acids of the N-terminal domain of IGF-binding protein-3 essential for high affinity IGF binding. J Clin Endocrinol Metab 86:4943–4950

5. **Hong J, Zhang G, Dong F, Rechler MM** 2002 Insulin-like growth factor (IGF)-binding protein-3 mutants that do not bind IGF-I or IGF-II stimulate apoptosis in human prostate cancer cells. J Biol Chem 277:10489–10497

6. **Spagnoli A, Torello M, Nagalla SR, Horton WA, Pattee P, Hwa V, Chiarelli F, Roberts Jr CT, Rosenfeld RG** 2002 Identification of STAT-1 as a molecular target of IGFBP-3 in the process of chondrogenesis. J Biol Chem 277:18860–18867

7. **Perks CM, McCaig C, Clarke JB, Clemmons DR, Holly JM** 2002 A non-IGF binding mutant of IGFBP-3 modulates cell function in breast epithelial cells. Biochem Biophys Res Commun 294:988–994

8. **Valentinis B, Bhala A, DeAngelis T, Baserga R, Cohen P** 1995 The human insulin-like growth factor (IGF) binding protein-3 inhibits the growth of fibroblasts with a targeted disruption of the IGF-I receptor gene. Mol Endocrinol 9:361–367

9. **Zadeh SM, Binoux M** 1997 The 16-kDa proteolytic fragment of insulin-like growth factor (IGF) binding protein-3 inhibits the mitogenic action of fibroblast growth factor on mouse fibroblasts with a targeted disruption of the type 1 IGF receptor gene. Endocrinology 138:3069–3072

10. **Rajah R, Valentinis B, Cohen P** 1997 Insulin-like growth factor (IGF)-binding protein-3 induces apoptosis and mediates the effects of transforming growth factor-beta1 on programmed cell death through a p53- and IGF-independent mechanism. J Biol Chem 272:12181–12188

11. **Silha JV, Sheppard PC, Mishra S, Gui Y, Schwartz J, Dodd JG, Murphy LJ** 2006 Insulin-like growth factor (IGF) binding protein-3 attenuates prostate tumor growth by IGF-dependent and IGF-independent mechanisms. Endocrinology 147:2112–2121

12. **Delbe J, Blat C, Desauty G, Harel L** 1991 Presence of IDF45 (mlGFBP-3) binding sites on chick embryo fibroblasts. Biochem Biophys Res Commun 179:495–501

13. **Oh Y, Muller HL, Pham H, Rosenfeld RG** 1993 Demonstration of receptors for insulin-like growth factor binding protein-3 on Hs578T human breast cancer cells. J Biol Chem 268:26045–26048

14. **Leal SM, Liu Q, Huang SS, Huang JS** 1997 The type V transforming growth factor beta receptor is the putative insulin-like growth factor-binding protein 3 receptor. J Biol Chem 272:20572–20576

15. **Huang SS, Ling TY, Tseng WF, Huang YH, Tang FM, Leal SM, Huang JS** 2003 Cellular growth inhibition by IGFBP-3 and TGF-β1 requires LRP-1. FASEB J 17:2068–2081

16. **Ricort JM** 2004 Insulin-like growth factor binding protein (IGFBP) signalling. Growth Horm IGF Res 14:277–286

17. **Fanayan S, Firth SM, Butt AJ, Baxter RC** 2000 Growth inhibition by insulin-like growth factor-binding protein-3 in T47D breast cancer cells requires transforming growth factor-β (TGF-β) and the type II TGF-β receptor. J Biol Chem 275:39146–39151

18. **Smith EP, Lu L, Chernausek SD, Klein DJ** 1994 Insulin-like growth factor-binding protein-3 (IGFBP-3) concentration in rat Sertoli cell-conditioned medium is regulated by a pathway involving association of IGFBP-3 with cell surface proteoglycans. Endocrinology 135:359–364

19. **Yang YW, Yanagishita M, Rechler MM** 1996 Heparin inhibition of insulin-like growth factor-binding protein-3 binding to human fibroblasts and rat glioma cells: role of heparan sulfate proteoglycans. Endocrinology 137:4363–4671

20. **Lee KW, Liu B, Ma L, Li H, Bang P, Koeffler HP, Cohen P** 2004 Cellular internalization of insulin-like growth factor binding protein-3: distinct endocytic pathways facilitate re-uptake and nuclear localization. J Biol Chem 279:469–476

21. **Singh B, Charkowicz D, Mascarenhas D** 2004 Insulin-like growth factor-independent effects mediated by a C-terminal metal-binding domain of insulin-like growth factor binding protein-3. J Biol Chem 279:477–487

22. **Radulescu RT** 1994 Nuclear localization signal in insulin-like growth factor-binding protein type 3. Trends Biochem Sci 19:278

23. **Li W, Fawcett J, Widmer HR, Fielder PJ, Rabkin R, Keller GA** 1997 Nuclear transport of insulin-like growth factor-I and insulin-like growth factor binding protein-3 in opossum kidney cells. Endocrinology 138:1763–1766

24. **Schedlich LJ, Young TF, Firth SM, Baxter RC** 1998 Insulin-like growth factor-binding protein (IGFBP)-3 and IGFBP-5 share a common nuclear transport pathway in T47D human breast carcinoma cells. J Biol Chem 273:18347–18352

25. **Schedlich LJ, Le Page SL, Firth SM, Briggs LJ, Jans DA, Baxter RC** 2000 Nuclear import of insulin-like growth factor-binding protein-3 and -5 is mediated by the importin β subunit. J Biol Chem 275:23462–23470

26. **Liu B, Lee HY, Weinzimer SA, Powell DR, Clifford JL, Kurie JM, Cohen P** 2000 Direct functional interactions between insulin-like growth factor-binding protein-3 and retinoid X receptor-α regulate transcriptional signaling and apoptosis. J Biol Chem 275:33607–33613

27. **Bhattacharyya N, Pechhold K, Shahjee H, Zappala G, Elbi C, Raaka B, Wiench M, Hong J, Rechler MM** 2006 Non-secreted insulin-like growth factor binding protein-3 (IGFBP-3) can induce apoptosis in human prostate cancer cells by IGF-independent mechanisms without being concentrated in the nucleus. J Biol Chem 281:24588–24601

28. **Butt AJ, Fraley KA, Firth SM, Baxter RC** 2002 IGF-binding protein-3-induced growth inhibition and apoptosis do not require cell surface binding and nuclear translocation in human breast cancer cells. Endocrinology 143:2693–2699

29. **Schedlich LJ, O'Han MK, Leong GM, Baxter RC** 2004 Insulin-like growth factor binding protein-3 prevents retinoid receptor heterodimerization: implications for retinoic acid-sensitivity in human breast cancer cells. Biochem Biophys Res Commun 314:83–88

30. **Ikezoe T, Tanosaki S, Krug U, Liu B, Cohen P, Taguchi H, Koeffler HP** 2004 Insulin-like growth factor binding protein-3 antagonizes the effects of retinoids in myeloid leukemia cells. Blood 104:237–242

31. **Heyman RA, Mangelsdorf DJ, Dyck JA, Stein RB, Eichele G, Evans RM, Thaller C** 1992 9-cis retinoic acid is a high affinity ligand for the retinoid X receptor. Cell 68:397–406

32. **Mangelsdorf DJ, Ong ES, Dyck JA, Evans RM** 1990 Nuclear receptor that identifies a novel retinoic acid response pathway. Nature 345:224–229

33. **Mangelsdorf DJ, Thummel C, Beato M, Herrlich P, Schutz G, Umesono K, Blumberg B, Kastner P, Mark M, Chambon P, Evans RM** 1995 The nuclear receptor superfamily: the second decade. Cell 83:835–839

34. **Kliewer SA, Umesono K, Mangelsdorf DJ, Evans RM** 1992 Retinoid X receptor interacts with nuclear receptors in retinoic acid, thyroid hormone and vitamin D3 signalling. Nature 355:446–449

35. **Kliewer SA, Umesono K, Noonan DJ, Heyman RA, Evans RM** 1992 Convergence of 9-cis retinoic acid and peroxisome proliferator signalling pathways through heterodimer formation of their receptors. Nature 358:771–774

36. **Mangelsdorf DJ, Evans RM** 1995 The RXR heterodimers and orphan receptors. Cell 83:841–850

37. **Chambon P** 1996 A decade of molecular biology of retinoic acid receptors. FASEB J 10:940–954

38. **Chawla A, Repa JJ, Evans RM, Mangelsdorf DJ** 2001 Nuclear receptors and lipid physiology: opening the X-files. Science 294:1866–1870

39. **Zusi FC, Lorenzi MV, Vivat-Hannah V** 2002 Selective retinoids and rexinoids in cancer therapy and chemoprevention. Drug Discov Today 7:1165–1174

40. **Clifford JL, Menter DG, Wang M, Lotan R, Lippman SM** 1999 Retinoid receptor-dependent and -independent effects of N-(4-hydroxyphenyl)retinamide in F9 embryonal carcinoma cells. Cancer Res 59:14–18

41. **Tarrade A, Bastien J, Bruck N, Bauer A, Gianni M, Rochette-Egly C** 2005 Retinoic acid and arsenic trioxide cooperate for apoptosis through phosphorylated RXRα. Oncogene 24:2277–2288

42. **Prufer K, Barsony J** 2002 Retinoid X receptor dominates the nuclear import and export of the unliganded vitamin D receptor. Mol Endocrinol 16:1738–1751

43. **Yasmin R, Williams RM, Xu M, Noy N** 2005 Nuclear import of the retinoid X receptor, the vitamin D receptor, and their mutual heterodimer. J Biol Chem 280:40152–40160

44. **Mangelsdorf DJ, Umesono K, Kliewer SA, Borgmeyer U, Ong ES, Evans RM** 1991 A direct repeat in the cellular retinol-binding protein type II gene confers differential regulation by RXR and RAR. Cell 66:555–561

45. **Ishaq M, Fan M, Natarajan V** 2000 Accumulation of RXRα during activation of cycling human T lymphocytes: modulation of RXRE transactivation function by mitogen-activated protein kinase pathways. J Immunol 165:4217–4225

46. **Boehm MF, Zhang L, Zhi L, McClurg MR, Berger E, Wagoner M, Mais DE, Suto CM, Davies JA, Heyman RA, Nadzan AM** 1995 Design and

synthesis of potent retinoid X receptor selective ligands that induce apoptosis in leukemia cells. J Med Chem 38:3146–3155

47. **Arnold JT, Le H, McFann KK, Blackman MR** 2005 Comparative effects of DHEA vs. testosterone, dihydrotestosterone, and estradiol on proliferation and gene expression in human LNCaP prostate cancer cells. Am J Physiol Endocrinol Metab 288:E573–E584

48. **Firth SM, Ganeshprasad U, Baxter RC** 1998 Structural determinants of ligand and cell surface binding of insulin- like growth factor-binding protein-3. J Biol Chem 273:2631–2638

49. **Angelloz-Nicoud P, Binoux M** 1995 Autocrine regulation of cell proliferation by the insulin-like growth factor (IGF) and IGF binding protein-3 protease system in a human prostate carcinoma cell line (PC-3). Endocrinology 136:5485–5492

50. **Xu L, Massague J** 2004 Nucleocytoplasmic shuttling of signal transducers. Nat Rev Mol Cell Biol 5:209–219

51. **Yin P, Xu Q, Duan C** 2004 Paradoxical actions of endogenous and exogenous insulin-like growth factor-binding protein-5 revealed by RNA interference analysis. J Biol Chem 279:32660–32666

52. **Wood WI, Cachianes G, Henzel WJ, Winslow GA, Spencer SA, Hellmiss R, Martin JL, Baxter RC** 1988 Cloning and expression of the growth hormone-dependent insulin-like growth factor-binding protein. Mol Endocrinol 2:1176–1185**Elbi C, Misteli T, Hager GL** 2002 Recruitment of dioxin receptor to active transcription sites. Mol Biol Cell 13:2001–2015

54. **Kroemer G, El-Deiry WS, Golstein P, Peter ME, Vaux D, Vandenabeele P, Zhivotovsky B, Blagosklonny MV, Malorni W, Knight RA, Piacentini M, Nagata S, Melino G** 2005 Classification of cell death: recommendations of the Nomenclature Committee on Cell Death. Cell Death Differ 12(Suppl 2):1463–1467

55. **van Engeland M, Nieland LJ, Ramaekers FC, Schutte B, Reutelingsperger CP** 1998 Annexin V-affinity assay: a review on an apoptosis detection system based on phosphatidylserine exposure. Cytometry 31:1–9

56. **Dingwall C, Laskey RA** 1991 Nuclear targeting sequences—a consensus? Trends Biochem Sci 16:478–481

57. **Cardin AD, Weintraub HJ** 1989 Molecular modeling of protein-glycosaminoglycan interactions. Arteriosclerosis 9:21–32

58. **Bach LA, Headey SJ, Norton RS** 2005 IGF-binding proteins—the pieces are falling into place. Trends Endocrinol Metab 16:228–234

59. **Schedlich LJ, Graham LD, O'Han M K, Muthukaruppan A, Yan X, Firth SM, Baxter RC** 2007 Molecular basis of the interaction between IGFBP-3 and retinoid X receptor: role in modulation of RAR-signaling. Arch Biochem Biophys 465:359–369

60. **Zhong C, Yang S, Huang J, Cohen MB, Roy-Burman P** 2003 Aberration in the expression of the retinoid receptor, RXRα, in prostate cancer. Cancer Biol Ther 2:179–184**Franklin SL, Ferry Jr RJ, Cohen P** 2003 Rapid insulin-like growth factor (IGF)-independent effects of IGF binding protein-3 on endothelial cell survival. J Clin Endocrinol Metab 88:900–907

62. **Liu B, Lee KW, Li H, Ma L, Lin GL, Chandraratna RA, Cohen P** 2005 Combination therapy of insulin-like growth factor binding protein-3 and retinoid X receptor ligands synergize on prostate cancer cell apoptosis in vitro and in vivo. Clin Cancer Res 11:4851–4856

63. **Lee KW, Cobb LJ, Paharkova-Vatchkova V, Liu B, Milbrandt J, Cohen P** 2007 Contribution of the orphan nuclear receptor Nur77 to the apoptotic action of IGFBP-3. Carcinogenesis 28:1653–1658

64. **Booth BA, Boes M, Andress DL, Dake BL, Kiefer MC, Maack C, Linhardt RJ, Bar K, Caldwell EE, Weiler J, Bar RS** 1995 IGFBP-3 and IGFBP-5 association with endothelial cells: role of C-terminal heparin binding domain. Growth Regul 5:1–17

65. **Fowlkes JL, Serra DM** 1996 Characterization of glycosaminoglycan-binding domains present in insulin-like growth factor-binding protein-3. J Biol Chem 271:14676–14679